

# Study the effect of Bauxite ceramic powder on the fracture mechanics of aluminum alloy using digital image correlation

Mohsin A. Aswad, Samir Hamid Awad, & Ali Hussein Kaayem

College of Materials Engineering / Department of Engineering of Ceramic and building materials, University of Babylon, Iraq.

\*Email: Mohsin.aswad@gmail.com

**ABSTRACT:** The modern research and industries have seen great interest in reinforcement of aluminum metal composites, AMMCs by ceramic particles due to their superior properties and applications. Digital image correlation, DIC method has proved its accuracy and effectiveness in tracking of crack initiation, propagation, and plastic deformation ahead the crack tip in fracture mechanics investigations. In this study, DIC was used to detect the surface strain and plastic deformation (necking) during tensile test of AMMCs reinforced using Iraqi natural bauxite ceramic powders (2-6% wt) with particle size of  $3.3\mu\text{m}$  using stir casting method. Also, the mechanical properties and fracture mechanics of AMMCs cast were investigated using extensometer method for comparison with DIC method. The results show maximum values for the ultimate tensile strength, yield strength, and Young's modulus (E) at 4% bauxite addition while the 6% addition exhibits the composite a nearly brittle behavior. Also, the hardness increases with bauxite increasing from 19.3 HBN for the aluminum matrix to 40.1 HBN for the AMMCs. DIC results could prove its superiority in comparison to the extensometer method as a suitable and very precise contactless method to identify the localized strain at the necking region and the plastic deformation at this region and the distribution of the brittle phases under tensile loading.

**KEYWORDS:** Aluminum matrix composite material, Bauxite ceramic powder, Fracture Mechanics, and Digital image correlation.

## INTRODUCTION

There are different methods to manufacture of the metal matrix composites, MMCs such as a continuous metallic matrix with discontinuous reinforcing phases like particulate, fiber, whiskers. Traditional materials are used in metal matrix composites in many applications, due to their superior properties for example high hardness, stiffness, wear, high strength to weight ratio, and corrosion resistance [1].

There are many applications for aluminum and its alloys due to their weight which gives them an additional advantages in many uses in engineering as: aerospace, automotive and military applications. Some of aluminum can be toughening with ceramics reinforcing materials for example  $\text{Al}_2\text{O}_3$ , SiC, SiC,  $\text{B}_4\text{C}$ , etc. because the unique properties as mentioned above [2,3].

The fracture strength of the composite specimens were improved by using one of the toughening mechanism which used particulate mechanism. This mechanism works to prevent the crack propagation through the aluminum composite matrix. The cracks were stopped and blocked or branching and splitting them, so the cracks progression across the composite specimen was delayed. The particle strengthening mechanism improve the mechanical properties such as stiffness and strength of the composite using the carrying a proportion of the load applied [4, 5].

The aluminum matrix composite properties are dependent on the reinforcement particles nature and the manufacturing process. The particle's strength and the strength of the interface between the matrix and particles lead to improve the fracture in particulate-reinforced composites. There are different types of failure will occur in the composite materials like de-bonding between matrix and particles, particulate fracture, near particulate fracture, near interface fracture, and the failure between the particulate agglomerations [5-7].

The extensometer process is not proper for observation the strain at the necking regions and plastic deformation around the necking region and cracks initiation within the necking region which created under tensile test. Also, using strain gauge was used for measuring the localized strain but it is not suitable for composite materials due to the strains can be different on the sample surface which depended on the composite synthesis, the vary of the

strain measurements is identified depending on the location of the strain gauge [8].

To overcome the obstacles are mentioned above for extensometer and strain gauge, precise strain measurements may be accomplished with non-contact optical technique specifically digital image correlation, DIC which used to observe the strain of the tensile sample to detect crack initiation. The DIC principle is to discovery matched area with precise regions between the window sizes or subsets in both deform and non-deform image by a correlation function. The precision of DIC technique depends on many factors for example subset size and image quality [9, 10].

In the previous studies, there are many researches were achieved the using DIC technique for materials testing in both non-metal and metal material, in specific the plastic materials due to exhibiting heterogeneous behavior and composite materials. Also, DIC was used to recognize the elastic properties and surface deformation from measurement of displacement and strain respectively [11]. The inelastic deformation creates in porous brittle ceramic owing to initiation and development of micro-voids. DIC technique was used to measure the brittle fracture in the ceramic materials like graphite, silicon carbide, and to measure intergranular fracture in alumina [12, 13].

The main objectives of this research are to improve the mechanical properties (tensile strength, yield strength, Young's modulus, and hardness) of Al alloy by addition of Iraqi bauxite ceramic as reinforcing particles due to the bauxite ceramics available at low cost. The aim of this work is to use digital image correlation technique to visualize the necking regions, plastic deformation, and crack initiation at necking regions under tensile test.

## EXPERIMENTAL PROCEDURES

### Starting Materials

The starting materials to prepare of AMMCs specimens were Al wires cuts to dimensions  $\text{Ø } 3 \times 10$  mm, Mg powders in particle size about  $56.05 \mu\text{m}$ , and Iraqi bauxite rocks as reinforcement. Aluminum wires were cleaned and washed. Bauxite rocks was ground to obtain the quasi-finished powders. After that the bauxite powders was washed, dried, and milled at 350 rpm for 8 hours using a planetary mill and fired at temperature  $1400 \text{ }^\circ\text{C}$ . The particle sizes of calcined bauxite powder was  $0.97 \mu\text{m}$ . The chemical composition is shown in table 1

**Table 1.** The chemical composition of the bauxite material.

Element	SiO <sub>2</sub>	Al <sub>2</sub> O <sub>3</sub>	Fe <sub>2</sub> O <sub>3</sub>	CaO	MgO
Percent %	21.31	54.78	1.48	0.05	0.02

### Specimen Preparation

Stir casting was used to prepare the AMMCs. Aluminum wires were melt in the graphite crucible using furnace at temperature about  $700 \text{ }^\circ\text{C}$ . The bauxite powder was pre-heated at temperature  $300 \text{ }^\circ\text{C}$  for 15 min before adding bauxite particles to the melted aluminum to avoid moisture contains. The weight bauxite particles were covered using Al foil and put it carefully to realize bauxite particles from air. Magnesium powders were added to the Al melted to enhance the wettability between the matrix and the reinforcement phase. Table 2 displays the experimental program of the weight percent to Al-Mg composite as matrix and bauxite as reinforcing. The samples preparation were accomplished at the laboratories of the University of Babylon/ College of Materials Engineering.

**Table 2.** Components of AMMCs.

Sample Code	Al, wt%	Mg, wt%	Bauxite, wt%
<b>Pure Al</b>	98	2	0
<b>Al+2% Bauxite</b>	96	2	2
<b>Al+4% Bauxite</b>	94	2	4
<b>Al+6% Bauxite</b>	92	2	6

The temperature of melted AMMCs was reduced to temperature below the liquidus temperature of Al matrix and

this semi-solid molten of AMMCs was mixed using stirrer blade at 870 rpm for 8 minutes. After that the semi-solid molten of AMMCs was heated to temperature above the liquidus temperature 850 °C for increasing the fluidity. The melt of AMMCs was poured into the casting mold which preheated at 250 °C for forming tensile specimen. Then, the cast specimen was machined and surface finished to prepare the dog bone specimen as shown in figure 1 and table 3 according to ASTM E8-99.

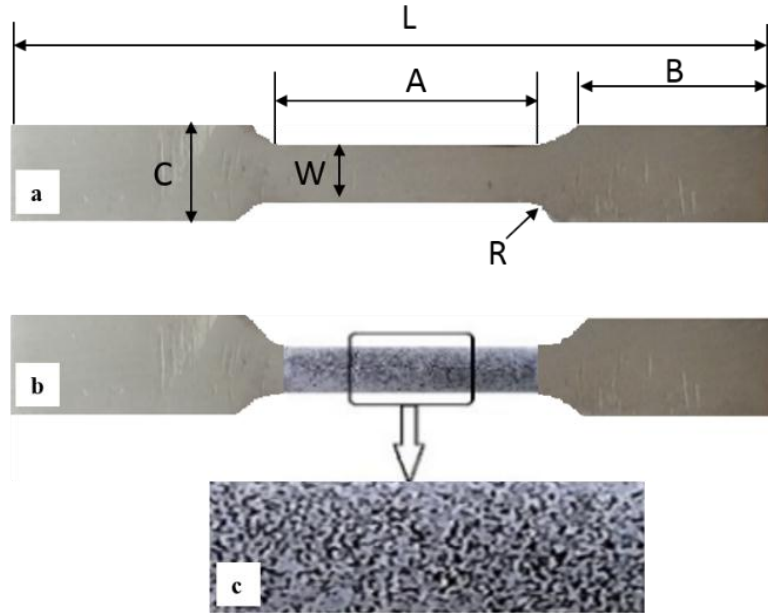


**Figure 1.** preparation steps of DIC sample (a) polished sample and (b) white paint spraying as a background; (c) make a subset on the sample.

**Table 3.** Specifications of the tensile specimen.

C- Width of grip section	19 mm
R- Radius of grip	12 mm
B- Length of grip section	48 mm
L- Overall length	180 mm
W- Width	12 mm
A- Length of reduced section	55 mm
G- Gage length	50 mm

#### Tensile Testing and DIC technique

The AMMCs samples with 50 mm gauge length was used in plane tension tests and achieved using universal tensile testing machine (Type WAW-200) under crosshead speed of about 2 mm/min. DIC algorithm can use to position the window size or subset to the non-deformed image and compare this image with series of deformed images. The DIC specimen was prepared by featuring its surface using a multilayer paint with a white background and black subsets to make the random speckle patterns on the samples surface to enable the tracking process as shown in figure 1C. One camera was used in this test owing to sufficient to observe the displacement and strain in the sample. A digital microscope camera was positioned in front of the sample at distance adjusted between the sample and the camera depending on the sample area to be measured as shown in figure 2. The camera resolution was set to 640 × 480 pixels and the length-pixel ratio of the imaging system is 0.0008 mm/pixel. The camera was planned to capture the pictures spontaneously at a mount rate 30 (30 images/sec), and this frame rate was appropriate to take and to store a large quantity of pictures for additional calculations. The contrast in the samples were enhanced and illuminated using light sources as shown in figure 2 and the localized strain of the

specimens were visualization during the tensile testing on the strain map. Furthermore, for comparison the strain results were measured depending on two methods, DIC and extensometer method. The electronic extensometer (YYL1-10/50-111276, Japan) was fixed on the samples as shown in figure 2 for recording its extension during the test, it was fixed to be in front to the reduced section of the sample.

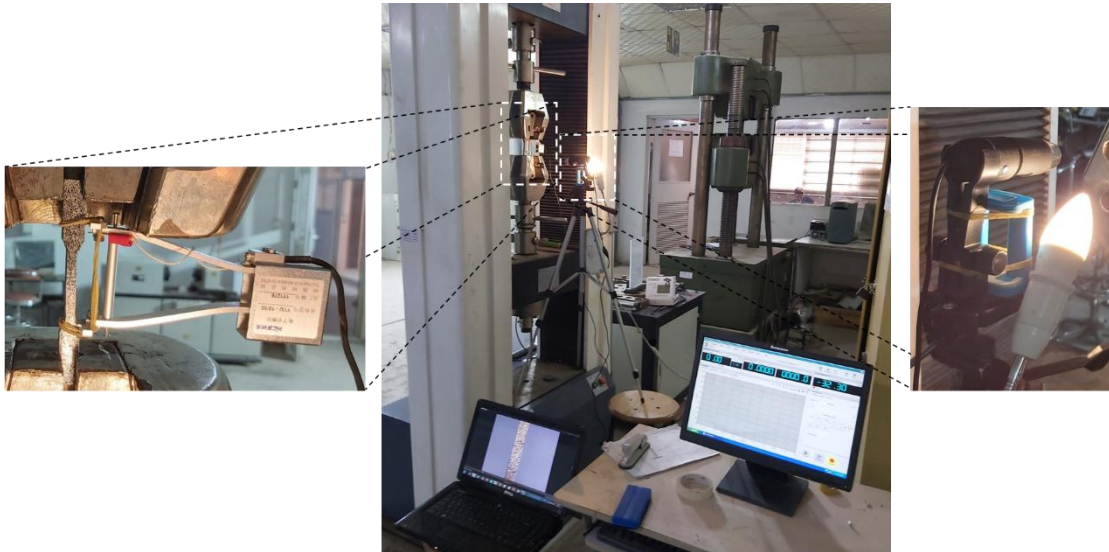


**Figure 2.** Setup of uniaxial tensile test. Illuminating the sample surface using lamp and digital image camera is located in front of specimen.

#### Determination of mechanical properties

The DIC strain was measured using DIC software. The software of DIC used for calculation named GOM (Gesellschaft für Optische Messtechnik) from a Germany company. The DIC calculation method begins with a non-deformed image captured before loading and then matched with a large number of images after loading intervals. The features on the samples surface within the subset was remaining before and after the deformation. The interrogation window size or the subset was used 29×29 pixels and overlap 15%. First the image divided to more of subsets and examine for the corresponding window sizes after distortion based on the hypothesis and calculates their displacements; lastly, a displacement or deformation distribution map is formed. The DIC strain was measured using line profile measured by the change the distance between the two points on the gauge length as shown in figure 8. The true strain, load-time curve, and stress-strain curve were determined using extensometer during the tensile test. The Hardness test was measured using Brinell hardness and Young's modulus, E was calculated using the ultrasonic device (CSI type CCT-4) according to the following equation 1:

$$E=2\rho Cs^2 (1+\nu) \quad \text{----- (1)}$$

Where: Cs is speed of sound of shear,  $\rho$  is density of the specimen, and  $\nu$  is Poisson's ratio.

## RESULTS AND DISCUSSION

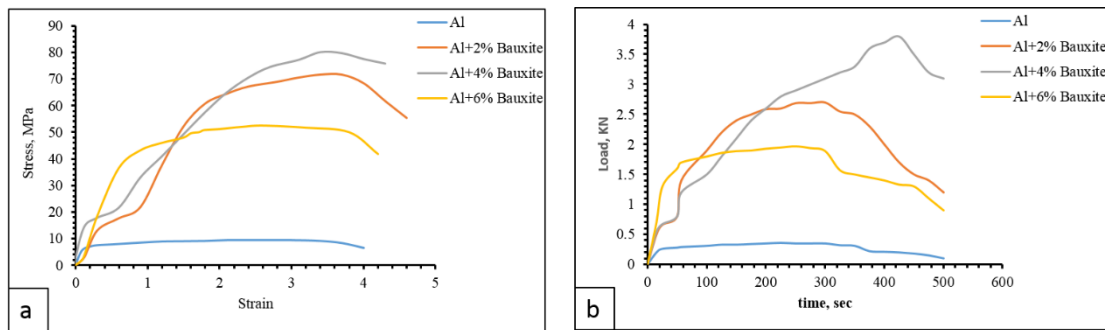
### Mechanical Properties

Figure (3-4), and table 3 shows the results of the mechanical properties of AMMCs samples reinforced with bauxite particles. It can be observed, that the strength by means of tensile strength, yield strength, Young's modulus, and hardness increased with increasing of the bauxite addition. Such improvement can be attributed to the role of bauxite particles which act to restrain the matrix movement in their vicinity and tend to restrict the dislocation motion.

**Table 3.** Mechanical properties of the AMMCs specimens.

Samples	Young Modulus, GPa	Yield Strength, MPa	Tensile Strength, MPa	Hardness, HBN, Kg/mm <sup>2</sup>
Pure Al	16.2	8.1	10.3	19.3
Al+2% Bauxite	22.2	52.2	72.3	30.2
Al+4% Bauxite	42.5	65.6	80.3	38.7
Al+6% Bauxite	33.2	43.3	52.5	40.1

The 4% of AMMCs samples could record maximum improvement (64%) in strength. However, the 6% of AMMCs samples showed the lowest mechanical properties among the other samples, probably, due to the agglomeration of bauxite particles which can cause a poor wettability between the bauxite powders and Al matrix. The hardness of AMMCs samples increased with increasing of bauxite addition, whereby, the hard bauxite particles act as barriers to matrix motion [14]. Figure 4 shows the comparison between the extensometer and DIC strains for the opening strain-time profile. The strain results of extensometer and DIC technique were found in good matching and agreement [11].



**Figure 3.** a) Relationship between the stress and strain, and b) Load and Time for different AMMCs specimens.

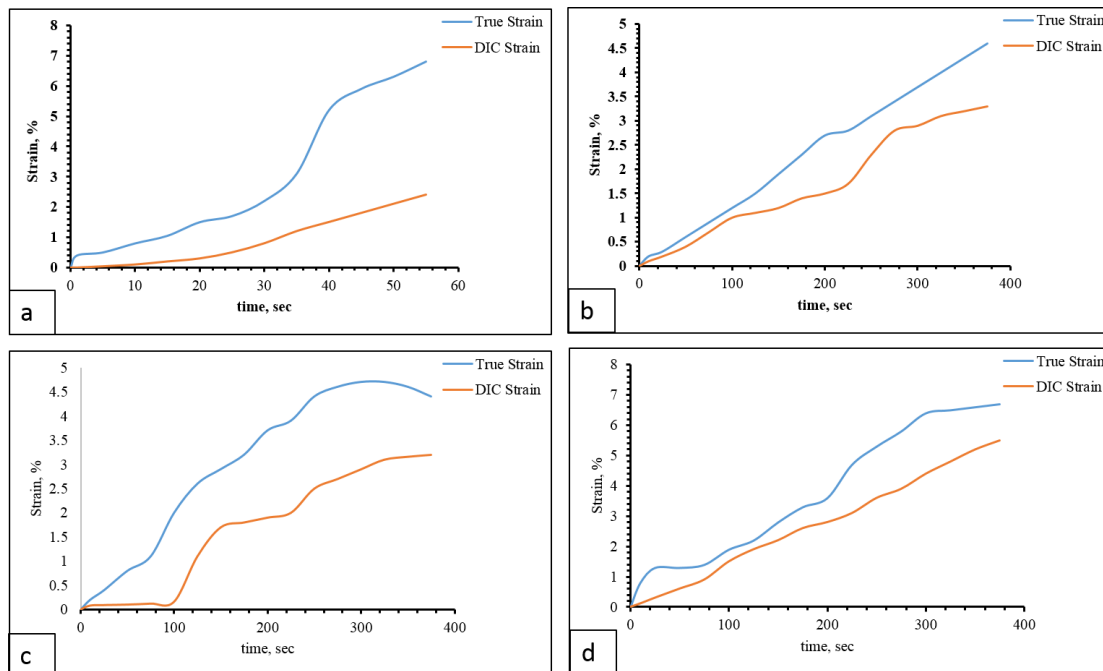


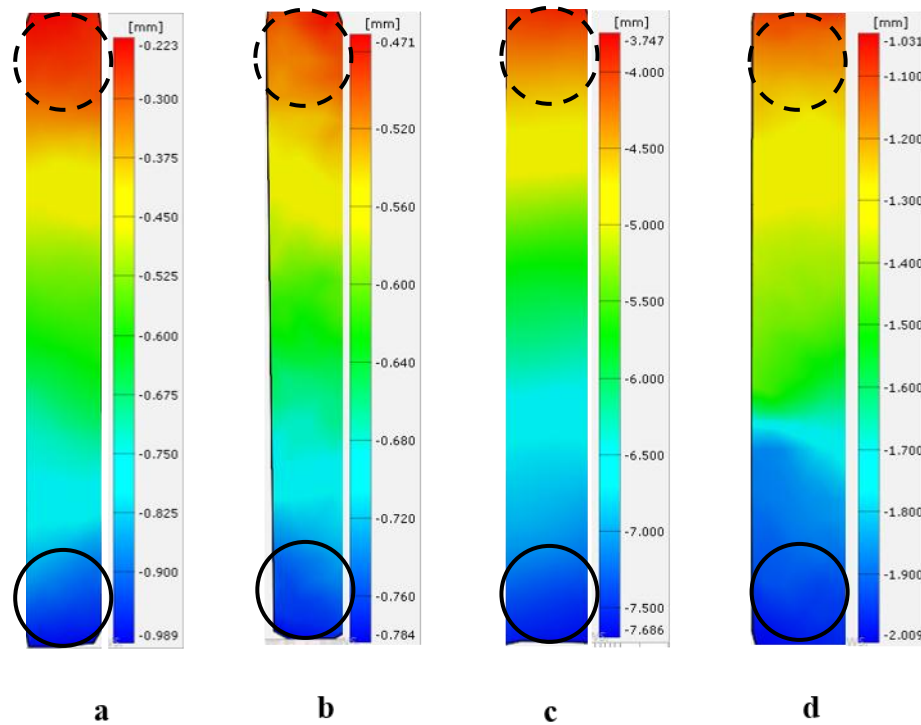
**Figure 4.** comparison between true & engineering strains from extensometer and DIC techniques for different AMMCs samples ; a) pure Al, b) Al+2%bauxite, c) Al+4%bauxite, and d) Al+6%bauxite.

## Digital Image Correlation results

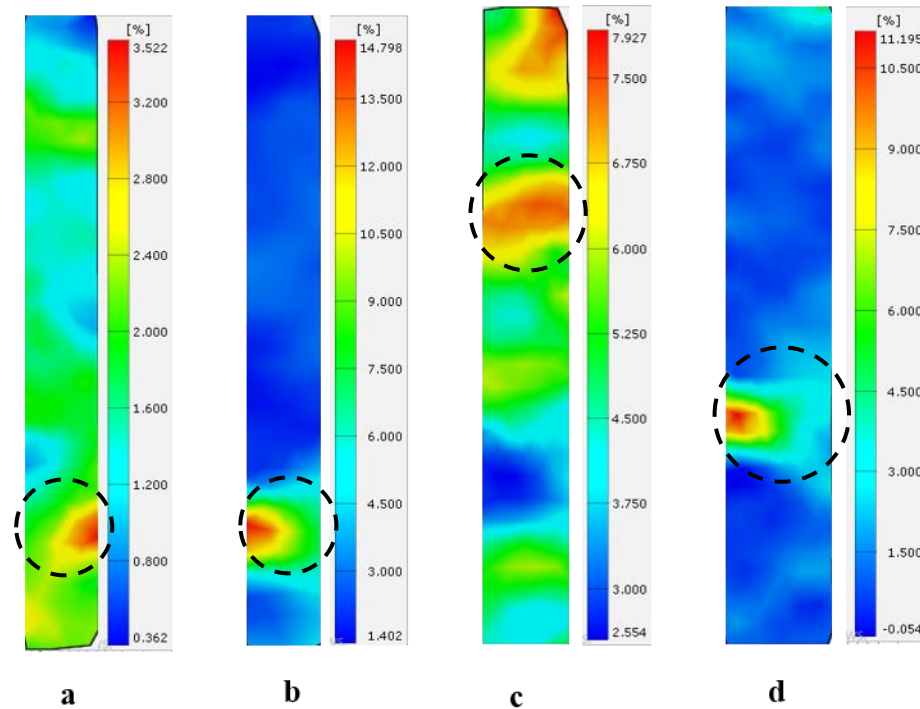
### Displacement and Strain Maps

Figure 5 shows the displacement maps for various AMMCs samples under tensile test, which showed the high displacement (red area) at the pulling edge but the fixed edge displayed very low displacement (blue area) as shown on the scale bars.

In plane, strains were obtained from DIC software. Figures (5-6) show the color contour of the axial logarithmic strain in Y-direction. The plastic deformation can be observed uniform at the gauge length of the AMMCs samples and it concentrated at the local region. This concentrated plastic deformation is called as necking. The necking of AMMCs can be divided into two types such as local necking and diffuse for initiation voids and then these voids will coalescences to form micro-crack which leads to the failure of samples. The strain concentration at thickness was higher than that in width direction in local necking region as shown in figure 6.



**Figure 5.** Displacement maps different AMMCs samples, a) pure Al, b) Al+2% Bauxite, c) Al+4% Bauxite, and d) Al+6% Bauxite, (○) and (⊖) represents low displacement high displacement region, respectively.



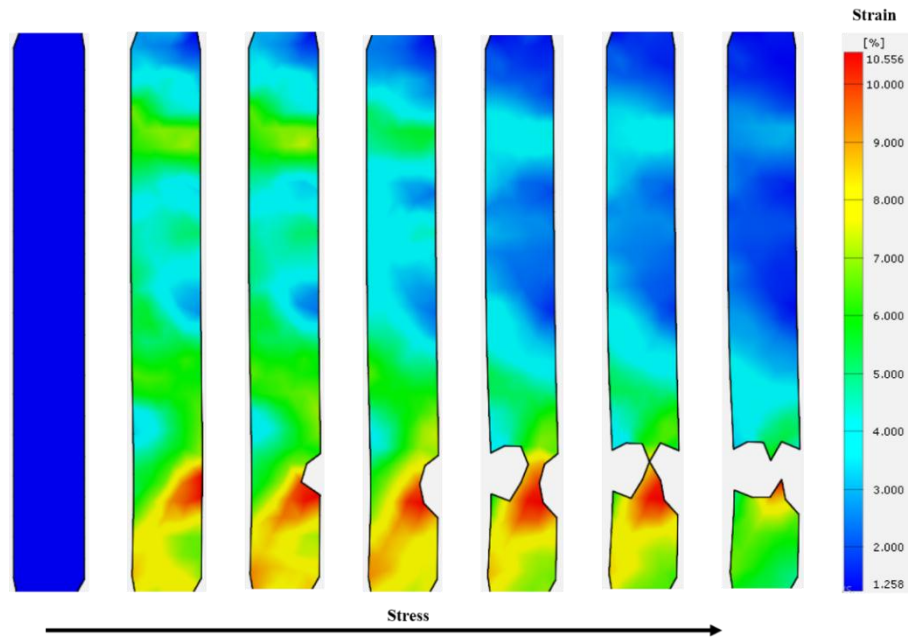
**Figure 6.** Strain maps for different AMMCs samples, a) pure Al, b) Al+2% Bauxite, c) Al+4% Bauxite, and d) Al+6% Bauxite.

#### Strain progression

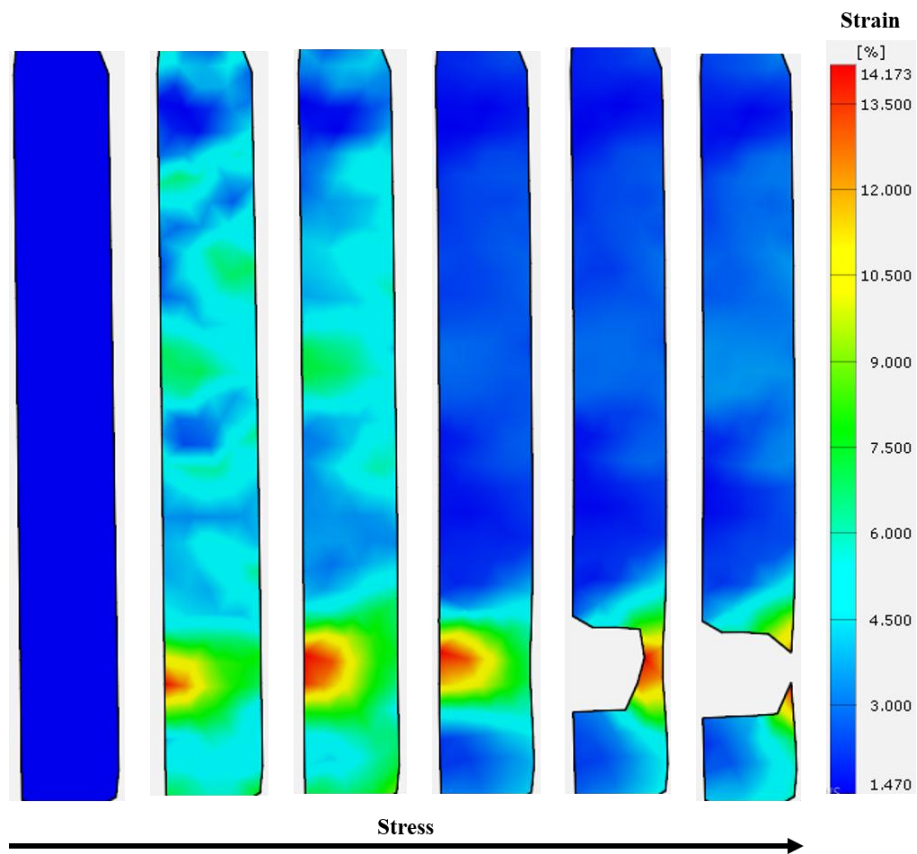
Figure 7 shows the major or opening strains with the different colors used to denote major strain changes for AMMCs samples. The map on the left shows the sample without any stress and strain but with increasing stress and time, the strain increased in uniform manner across the interested area of the specimens. Figure 7a shows the strain distribution in pure Al samples verified by plastic deformation as shown in the necking regions. The failure initiates at the necking area as voids and then these voids propagate to form microcracks which stress increases the microcracks propagate leads to failure the sample. Figure 7b represents the strain distribution for (Al+2% bauxite) samples which increased with increasing stress but the failure at the necking region was different from this of pure Al samples due to increase of the brittle phase [15].

Figure7 give the full field strain images at stress consecutive intervals, to show how the strain progresses through the material and the contour images of the maximum strain calculated by DIC at different time period throughout the tensile test for AMMCs samples. The right color bar of each image indicates the percent values of the strains. The necking regions represents the high strains and necking in AMMCs under tensile test after the flow stress is larger than the work hardening rate. The reasons of this case due to the maximum load on the load-displacement curve, well in the necking region before fracture and the micro cracks initiated in the sample [16].





a)



b)

**Figure 7.** The progression of strains in the AMMCs samples of the tensile test, a) pure Al, b) Al+2% Bauxite.

Crack Opening analysis and displacement method

Figure 8 shows the typical profile of the opening strain or crack opening in y-direction over time along the line profile at various points (A, B, and C) at different time periods through the tensile tests for pure Al. The crack



opening measurements have an individual line profile as shown in Figure 8a. The opening strain measured by differentiation with respect to distance using DIC program, can be completed to produce a smoothed Y-direction strain profile. Localized strain at the necking region can be identified in all samples as shown at point B on the figure 8a but the strains far away of the necking region at points A and C are negligible and the crack opening and necking are quite well identified on the figure. Figure 8b shows also that the opening strain increased with increasing time due to increasing the applied stress. Figure 9 represents the strain opening or crack opening for (Al+6% of bauxite) samples. Figure 10 represents the displacement in Y-direction for all samples, this figure shows that the displacement decreased with increasing bauxite additive due to increase the elasticity, E and the strength of the composite specimens [17, 18].

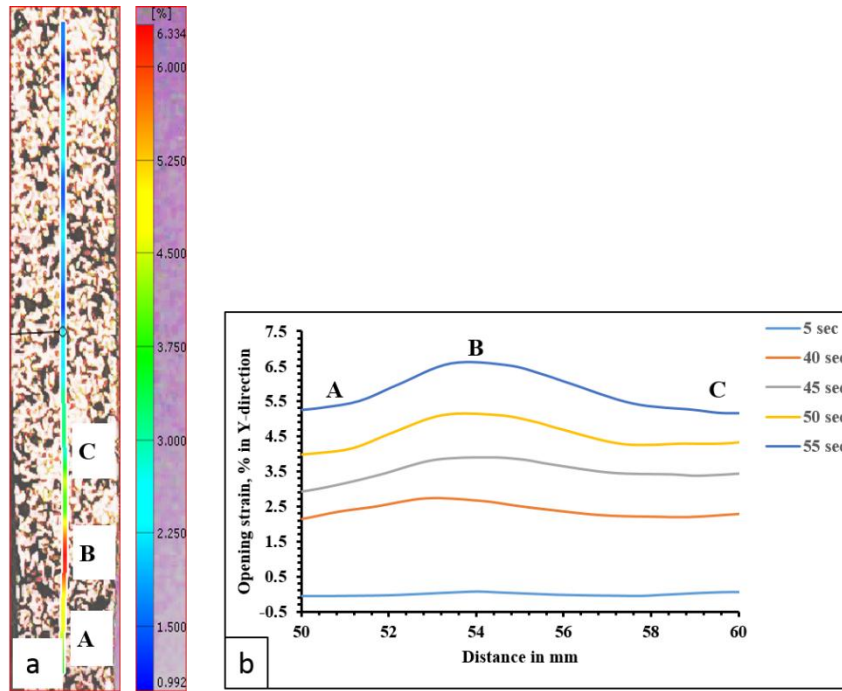


**Figure 8.** Shows the opening strain crack opening over time for pure Al samples, a) line profile A to C, and b) opening strain in Y-direction versus time.

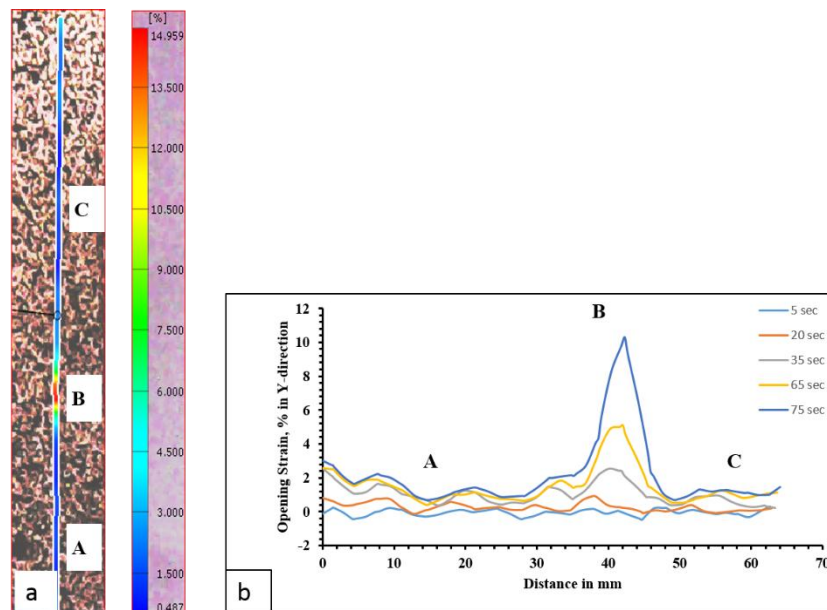


**Figure 9.** Shows the opening strain crack opening over time for (Al+6% bauxite) samples, a) line profile A to C, and b) opening strain in Y-direction versus time.

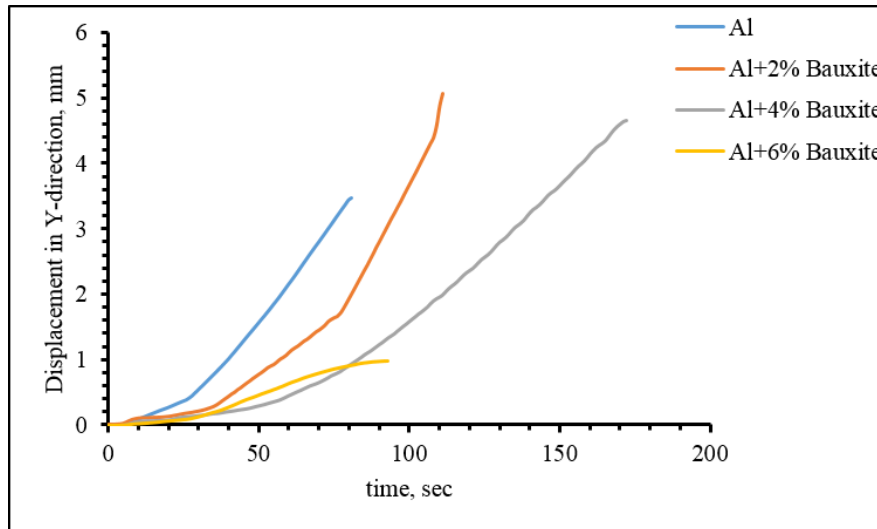


**Figure 10.** Shows the relationship between the displacements in Y-direction versus time for different AMMCs samples.

## CONCLUSIONS

The AMMCs reinforced with Iraqi natural bauxite ceramic particles were successfully prepared using stir casting method which is a good casting method. Tensile test was used to observe the failure and deformation in AMMCs specimens. A non-contact optical method was used to measure the displacement and surface strain through the necking region under tension by DIC and also, extensometer technique was used to measure the average strain.

The present study could strongly prove the activity of DIC in the accurate observation of localized strains and tracking of the crack origination and extension in the necking region in comparison to the extensometer technique. The average strain with digital image correlation as well as the values measured in extensometer method are in a good agreement.

The bauxite particles showed clear improvement in the mechanical properties of the AMMCs. Also, the reinforcement with 4% wt bauxite recorded the best results in the mechanical properties of the AMMCs.

## REFERENCES

- [1] S.M. Amel, " Iraqi Bauxite and Porcalinite Rocks Based Refractory, Preparation and Studying Properties", *Al-Khwarizmi Engineering Journal*, Vol. 13, No.2, 2017.
- [2] B. Rabindra, S. Das1, D. Chatterjee, G. Sutradhar, "Forgeability and Machinability of Stir Cast Aluminum Alloy Metal Matrix Composites", *Journal of Minerals & Materials Characterization \_ Engineering*, Vol. 10, No. 10, 2011.
- [3] U.B. Gopal Krishna, K.V. Sreenivas Rao & Vasudeva B," Effect of Boron Carbide Reinforcement on Aluminum Matrix Composites", *International Journal of Metallurgical \_ Materials Science and Engineering (IJMMSE)* ISSN 2278-2516, Vol. 3, No. 1, 2013.
- [4] S. Rama Rao, G. Padmanabhan, "Fabrication and mechanical properties of aluminum-boron carbide composites", *International Journal of Materials and Biomaterials Applications*, 2012.
- [5] A. Sallahuddin, N. Madeva, H.N. Reddappa and V. Auradi, "A Review on Particulate Reinforced Aluminum Metal Matrix Composites", *Journal of Emerging Technologies and Innovative Research (JETIR)*, Volume 2, No. 2, 2015.
- [6] L. Zaido, L. Nathalie, T. Amina, Q. Philippe, Jean-Francois Witz, and David Balloy, "Damage investigation in A319 aluminum alloy by digital image correlation during in-situ tensile tests", *21st European Conference of Fracture ECF21, 20-24 June 2016, Catania, Italy*. 2016.
- [7] Akira KATO, "Measurement of strain distribution in metals for tensile test using digital image correlation

- method and consideration of stress-strain relation", *Journal Engineering Journal*, Vol. 3, No.6, 2016.
- [8] S. M. Zeeshan, T. Fawad, N. Nausheen, A. M. Fahad, "Determination of Young's Modulus of Metallic and Composite Materials by Digital Image Correlation", *Journal of Space Technology*, Vol 1, No. 1, July 2012.
- [9] S. Liang, Z. Xiangchun, Z. Lu, W. Chiquan, W. Juntao, "Application of digital image correlation technique in stress and strain measurement", *15th Asia Pacific Conference for Non-Destructive Testing (APCNDT 2017)*, Singapore.
- [10] X. Feng, " Quantitative characterization of deformation and damage process by digital volume correlation: A review ", *Theoretical & Applied Mechanics Letters*, vol. 8, pp. 83-96, 2018.
- [11] Murat AYDIN, O.Z. Özkan, "Application of Digital Image Correlation Technique to Tensile Test for Printed Pla Specimens", *International Journal of 3D Printing Technologies and Digital Industry*, vol. 2, no. 2, pp. 1-7, 2018.
- [12] M. V. Grigorieva), V. V. Kibitkin, N. L. Savchenko, and V. R. Utyaganova, "In situ Study of Mechanical Damage Evolution of Segmented Ceramic Using Digital Image Correlation ", *Conference Paper in AIP Conference Proceedings November 2019*.
- [13] N. L. Savchenko, V. V. Kibitkin, and M. V. Grigoriev, " Characterization of Deformation and Damage Process of Alumina-Based Ceramics by DIC Technique", *Proceedings of the International Conference on Advanced Materials with Hierarchical Structure for New Technologies and Reliable Structures 2019*.
- [14] G. Karthikeyan, T.R. Jinu Gowthami, " Mechanical Properties and Metallurgical Characterization of LM<sub>25</sub>/ZrO<sub>2</sub> Composites Fabricated by Stir Casting Method", *revista Matéria*, Vol. 24, No. 3, 2019.
- [15] S.G. Miss Supriya, and R.R. Navthar, "Digital Image Correlation Technique for Strain Measurement of Aluminium Plate", *International Journal of Engineering Trends and Technology (IJETT)* – Vol. 39, No. 6- September 2016.
- [16] C. Yajun, J. Chunming, Z. Changtian, and S. Shengjie, "The Application of DIC Technique to Evaluate Residual Tensile Strength of Aluminum Alloy Plates with Multi-Site Damage of Collinear and Non-Collinear Cracks", *Metals* 2019, 9, 118; doi:10.3390/met 9020118.
- [17] M.A. Aswad, T.J. Marrow, "Intergranular crack nuclei in polycrystalline alumina", *Engineering Fracture Mechanics*, vol. 95, pp. 29–36 (2012).
- [18] A.J. Mohammed M. Hussien, A.A.Mohsin, and Hayder K. Rashed, "Investigation of crack propagation and opening in Hydroxyapatite using digital image correlation", *Journal of Engineering and Applied Science 12 (special no. 6)*: pp. 7935-7943, 2017.